JOURNAL OF GEOPHYSICAL RESEARCH, VOL. 103, NO. B12, PAGES 30,561-30,574, DECEMBER 10, 1998

Thermoremanent magnetization of nonuniformly magnetized grains

David J. Dunlop

Geophysics, Physics Department, University of Toronto, Toronto, Ontario, Canada

Abstract. A simple and elegant interpretation of thermoremanent magnetization (TRM) in uniformly magnetized single-domain (SD) grains was given by Néel 50 years ago, but the TRM acquisition processes in larger, nonuniformly magnetized grains are more varied and difficult to describe theoretically. SD TRM is a frozen high-temperature partition between two microstates: spins parallel or antiparallel to an applied magnetic field. Nonuniformly magnetized grains have a much greater choice of microstates (local energy minimum or LEM states), and partitioning among various LEM states continues to change during cooling. These changes may involve Barkhausen jumps of domain walls between positions of minimum local energy or nucleation of new domains and walls. Because of the lower remanence capacity of nonuniform microstates compared to the uniform SD state, TRM intensity decreases as grain size increases, although certain microstates, e.g., single-vortex states, seem to contribute little to TRM. Thermal demagnetization of TRM begins just above room temperature and continues to the Curie point, quite unlike the sharp "unblocking" of SD TRM. This continuous demagnetization, resulting from changes in microstates driven by the changing internal demagnetizing field during heating, profoundly affects the separation of different components of natural remanent magnetization and the determination of paleomagnetic field intensity.

1. Introduction

Thermoremanent magnetization (TRM) is acquired as a result of cooling from the Curie temperature T_C to room temperature T_0 in an applied magnetic field $\mathbf{H_0}$. At T_C, even a weak field will saturate a grain. During cooling, before TRM blocking begins, this single-domain (SD) state evolves first into fluctuating "predomain states" [*Ye and Merrill*, 1995] with only short-range order, then into more conventional structures. Depending on grain size, these may be nonuniform spin structures containing single or multiple vortices, few-domain structures with pseudo-single-domain (PSD) aspects to their behavior, or multidomain (MD) structures with domain wall displacements limited by self-demagnetization. Each of these structures acquires TRM in a different way. Vortex moments block in quasi-SD fashion and TRM is a partition between vortex-line moments parallel and antiparallel to $\mathbf{H_0}$. MD grains owe their TRM to pinned walls, which make a series of jumps during zero-field heating (multiple unblocking temperatures). PSD grains combine both styles of TRM.

Theorizing about TRM in nonuniformly magnetized grains is complicated by changes in domain structure below the original blocking temperature. Such transdomain changes often involve the nucleation or denucleation of domains during cooling. Each change alters the internal demagnetizing field, causing previously pinned walls to move. TRM is ultimately fixed only below the lowest temperature for transdomain changes. Transdomain changes in small grains, e.g., SD to two-domain (2D) or 2D to metastable SD or vortex, are particularly interesting because they could produce abrupt changes in the direction as well as the magnitude of TRM.

Paper number 98JB00026.
0148-0227/98/98JB-00026$09.00

TRM in grains which remain SD throughout their cooling to T_0 was interpreted by *Néel* [1949] as a frozen high-temperature partition between two microstates in which all spins are either parallel or antiparallel to an applied field $\mathbf{H_0}$. A similar approach can be taken to nonuniformly magnetized grains except that the partitioning is among a greater variety of microstates and the energy barriers between states may be difficult to calculate because of the complex transformation modes. The purpose of the present paper is to review current theories and the available TRM data in the light of these ideas.

2. Single-Domain TRM

An SD grain contains a single magnetic domain, with a spontaneous magnetization $\mathbf{M_s}$ resulting from the parallel exchange coupling of atomic spins. The magnetic moment $V\mathbf{M_s}$, where V is the volume of the grain, has a choice of orientations dictated by easy axes of crystalline or shape anisotropy. Shape anisotropy is usually dominant in minerals like magnetite with a high M_s and produces two energy minima, corresponding to spins in one or other direction along the longest axis of the grain. These are the two SD microstates.

Perfectly parallel coupling of spins is not maintained in all situations. During a transformation between the microstates (an SD reversal), the structure may be temporarily nonuniform (noncoherent reversal modes). Furthermore, at all temperatures above 0 K, thermal excitations perturb the spin lattice. Reversal of a single spin is one possible excitation, but a much lower energy perturbation is a spin wave, in which spins "precess" spatially on the surface of a cone. As the temperature T increases, spin waves with larger cone angles can be excited and $M_s(T)$ decreases steadily. At high T, reversals of grain moments are also excited and $M_s(T)$ drops rapidly to zero at the Curie temperature T_C. Even above T_C, where the system is nominally paramagnetic, short-range order persists,

showing that exchange coupling has not been completely destroyed.

For some tens of degrees below T_C, SD reversals are frequent on ordinary timescales. This condition is known as superparamagnetism because quite small fields $\mathbf{H_0}$ will align the moments of different SD grains and produce a strong magnetization **M**. The magnetic field energy, $E_H = -\mu_0 V \mathbf{M_s}.\mathbf{H_0}$, is dominant at these temperatures. A remanent magnetization in zero field only becomes possible when the demagnetizing energy $E_d = \frac{1}{2}\mu_0 V N M_s^2$ (N is demagnetizing factor, determined by the shape of the grain) increases with cooling sufficiently to provide a shape anisotropy barrier against SD reversals (Figure 1). The transition from superparamagnetism to stable remanence is quite sharp and occurs at the blocking temperature T_B [*Néel*, 1949].

During further cooling from T_B to T_0, the energy barriers ΔE_{12}, ΔE_{21} grow and few if any transitions occur between microstates 1 and 2, with $V\mathbf{M_s}$ parallel or antiparallel to $\mathbf{H_0}$. The only change in magnetization is a reversible increase in intensity due to the growth in $M_s(T)$ with cooling. Thus TRM at T_0 is essentially a frozen high-temperature Boltzmann partition between competing microstates 1 and 2.

These are the essential elements of *Néel*'s [1949] theory, and they lead to three main quantitative predictions. First, M (measured in the direction of $\mathbf{H_0}$) varies with time t as

$$M(t) = M_{eq} + (M_0 - M_{eq}) \exp(-t/\tau), \quad (1)$$

where M_0 is the initial magnetization before a change in field $\mathbf{H_0}$ and M_{eq} is the equilibrium magnetization long after the field change. Equation (1) is the kinetic equation describing the relaxation of M toward equilibrium due to transitions between the microstates.

Néel's second prediction is that the relaxation time τ is related to absolute temperature T and microcoercivity H_K by

$$1/\tau = C \exp(-\Delta E_{21}/kT)$$

$$= C \exp[-(\mu_0 V M_s H_K/2kT)(1 - H_0/H_K)^2], \quad (2)$$

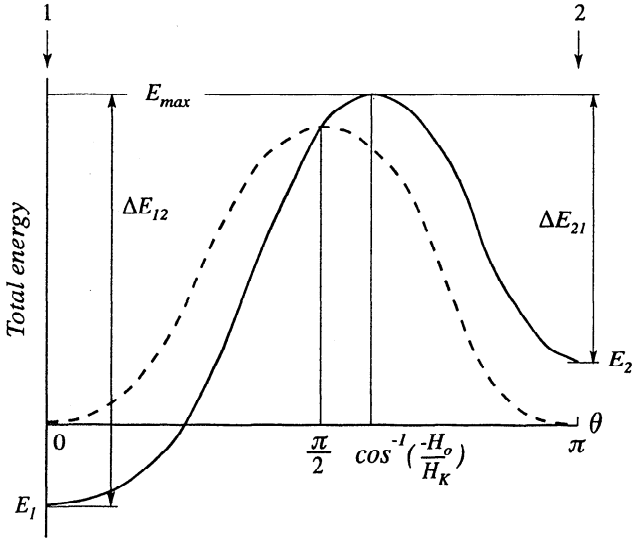

Figure 1. Energy barriers ΔE_{12} and ΔE_{21} for transitions between states 1 and 2 of an SD grain (SD and SD′, **M** parallel or antiparallel to $\mathbf{H_0}$). The total energy is the sum of E_d and E_H. E_1 is less than E_2 because $\mathbf{H_0}$ favors state 1. When $H_0 = 0$, the states are equivalent (dashed curve).

$C = 10^9$–10^{10} s^{-1} being the attempt frequency for transitions between microstates and k being Boltzmann's constant. (Strictly speaking, transitions from state 1 to state 2 across the energy barrier ΔE_{12} should also be included, but changes from 2 to 1 are strongly favored by $\mathbf{H_0}$.) Because the relaxation time depends exponentially on T, there is a well-defined blocking temperature T_B above which M relaxes almost instantaneously to M_{eq} but below which M is frozen or blocked at its initial value. Below T_B, $\mathbf{H_0}$ can be removed with no change in M.

Thus SD TRM is blocked at T_B during cooling. Conversely, TRM will survive reheating from T_0 in zero field until T_B, at which temperature it will unblock or demagnetize completely. The unblocking temperature T_{UB} during heating is the same as the blocking temperature T_B during cooling if the field H_0 is weak.

Néel's third prediction is that the thermal equilibrium magnetization M_{eq} above and at the blocking temperature is

$$M_{eq} = \Sigma M_i \exp(-E_i/kT) / \Sigma \exp(-E_i/kT)$$

$$= M_s \tanh(\mu_0 V M_s H_0/kT), \quad (3)$$

$M_1 = M_s$, $M_2 = -M_s$ being the magnetizations of the field parallel and antiparallel microstates, respectively, and the microstate energies E_1, E_2 being the sum of E_H and E_d (see Figure 1). Since M_{eq} is frozen below T_B, equation (3) also describes TRM at T_0. In particular, it predicts the dependence of TRM intensity on field strength H_0.

3. Above the SD Threshold: LEM States

The critical SD size d_0, the threshold between SD and non-SD states, is determined largely by M_s. Hematite has a small M_s value (≈2 kA/m at T_0) and a large d_0 (≈15 μm). Néel's [1949] SD theory is therefore relevant to TRM in many naturally occurring hematites. Titanomagnetite with ~60 mol % Ti (TM60) and pyrrhotite have critical SD sizes around 1 μm. Néel SD TRM theory is only relevant to submicroscopic grains of these minerals. Magnetite, the commonest carrier of natural remanent magnetization (NRM) in nature, has a strong M_s (480 kA/m at T_0) and a small d_0 of ~0.1 μm. Néel SD theory has little direct relevance to TRM in naturally occurring magnetites, apart from very elongated crystals or chains of crystals.

In reality, the grain size limits separating uniform SD structures and nonuniformly magnetized structures are not hard and fast. There is a size range over which grains, depending on their magnetic history, may adopt either type of structure, e.g., SD or two-domain (2D) (Figure 2). The alternative types of structures are called local energy minimum (LEM) states [*Moon and Merrill*, 1984], and the LEM state of lowest energy is the global energy minimum (GEM) state.

Although LEM states other than the GEM state are in principle metastable, they can be very long-lived, depending on the energy barriers between microstates. Above d_0, 2D is the GEM state. Transitions from SD to 2D require an activation energy $\Delta E_{12} = E_{max} - E_{SD}$ and are much easier than transitions from 2D to SD, which must surmount an energy barrier $\Delta E_{21} = E_{max} - E_{2D}$ (Figure 2). Provided thermal energy of at least ΔE_{12} is available, grains will tend to revert to the 2D GEM state. At any instant, there may be a significant population excited to the SD state, but these will not be long-lived states. Only if the thermal energy is insufficient for escape from the SD state, i.e., $< \Delta E_{12}$, will some grains remain trapped in metastable SD states. Such states have been observed in

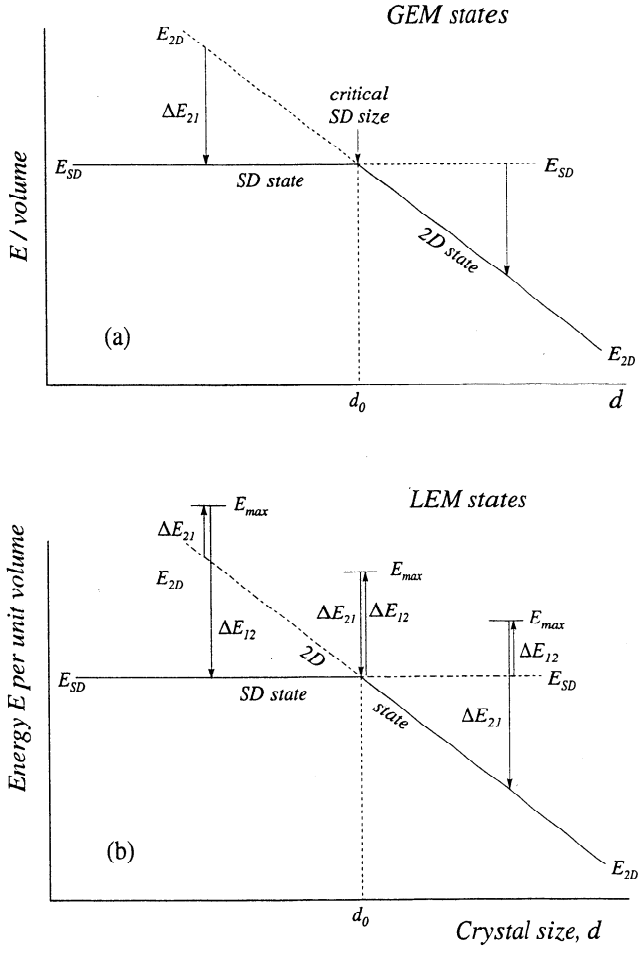

Figure 2. (a) Old and (b) modern pictures of magnetic microstates. In the old picture, only the lowest energy state (the GEM state) is occupied and transitions from a higher-energy state occur spontaneously, releasing energy ΔE_{21} or ΔE_{12}. In the modern picture, the crystal has a choice of alternative microstates (LEM states), in this example SD and 2D. Transitions are controlled by the barrier energy E_{max} between LEM states. For example, in an SD grain larger than critical SD size d_0, energy $\Delta E_{12} = E_{max} - E_1$ must be supplied to reach the top of the barrier and energy ΔE_{21} is then released in the transition to the 2D state. If energy ΔE_{12} is not available, the grain will remain in a metastable SD state. Below a limiting size, the energy barrier $\Delta E_{21} \rightarrow 0$ and the 2D state destabilizes, while above another limiting size, $\Delta E_{12} \rightarrow 0$ and the SD state destabilizes. Only between these limits is there a choice of LEM states.

grains of pyrrhotite, TM60 and magnetite much larger than critical SD size [*Halgedahl and Fuller*, 1983; *Boyd et al.*, 1984].

Very frequently there is enough thermal energy available to permit transitions out of the excited state. Grains then spend most of their time in the GEM or ground state. Notice also in Figure 2 that there are limits to the size range over which grains have a choice of states. The coexistence range changes with temperature (usually it narrows at high temperature), with the result that smaller grains may be forced into the SD ground state (because E_{max} becomes equal to E_{2D} and the barrier ΔE_{21} disappears), while larger grains will be forced into 2D states.

The general tendency for nonuniform magnetization states of lower remanence capacity to dominate as the grain size increases accounts for the experimental observation that TRM intensity, M_{tr}, decreases steadily above the SD threshold. In magnetite, for instance, M_{tr} decreases almost 2 orders of magnitude between 0.1 and 10 μm (Figure 3). This ~1/d size dependence of M_{tr} is one of the basic experimental constraints on TRM theories for nonuniformly magnetized grains.

4. TRM Acquisition

Let us follow the TRM acquisition process, starting from T_C (580°C for magnetite). Very close to T_C, where $M_s \rightarrow 0$, E_H outweighs any other long-range energy term. (The exchange energy, which describes coupling of neighboring spins, ensures short-range order, even above T_C, but not long-range order, i.e., domains.) E_H becomes dominant because it decreases with increasing T as $M_s(T)$, whereas other energies decrease more rapidly: E_d as $M_s^2(T)$, crystalline anisotropy energy E_K as $M_s^6(T)$ [*Sahu and Moskowitz*, 1995], and so on. Thus near T_C, a weak field $\mathbf{H_0}$ will saturate even a large grain, producing an SD state (Figure 4, top). Because of the large thermal excitation energy, the SD state (and domains generally) do not have parallel spins at these very high temperatures, but they are simple spin wave modes with no reversed spins.

Ye and Merrill [1995] consider that within a degree or so below T_C there exist thermally excited and constantly changing "predomain states," which they model by fractal modes in which individual spins or groups of spins are reversed to the field-favored direction of the bulk of the spin lattice. Such predomain states are appealing because they introduce an element of randomness that is absent in other more deterministic TRM models. If the regions of reversed spins could be stabilized by cooling, they might nucleate full-scale reverse domains at lower temperatures and explain the observed variability of TRM states in replicate coolings of individual TM60 grains (Figure 5).

However, there are objections to *Ye and Merrill*'s [1995] model. Although structures with short-range order exist above T_C, they are likely to be complicated superpositions of spin wave modes, including some reversed modes. These are less suitable predomain nuclei than the discrete spatial blocks of reversed spins imagined by Ye and Merrill. Furthermore, it is not clear that either type of short-range ordered structures can persist even a degree or two below T_C, let alone 10-20°C below T_C in the range of typical TRM blocking temperatures. T_C marks the sharp onset of long-range order and, in the presence of even a weak field, the appearance of ordered domain-scale structures with a regular rather than an irregular spacing.

We shall assume that any predomain structures present at T_C are rapidly damped with cooling and merge with conventional domain structures. A picture of evolving LEM states based on one-dimensional micromagnetic calculations appears in Figure 4. The microstates appear as local minima in the total energy surface, which is plotted in terms of the spin angles at the left and right surfaces of the grain [*Enkin and Dunlop*, 1987]. The SD microstate is located at (0°,0°), with spins at the left and right (and throughout the lattice between) at 0° to $\mathbf{H_0}$. (More precisely, the axis of the spin cone is at 0° to $\mathbf{H_0}$ throughout the grain.) The reversed SD state (SD′) would be at (180°,180°), outside the mapped area. At 579°C, SD and SD′ are the only LEM states, but by 578°C, a 2D state has developed near (180°,0°). In fact, its energy is lower than SD: 2D is now the GEM state.

SD reversals, SD→SD′, now occur via an intermediate 2D resting state, along the transition path shown. The SD→2D transformation is called a transdomain transition because the

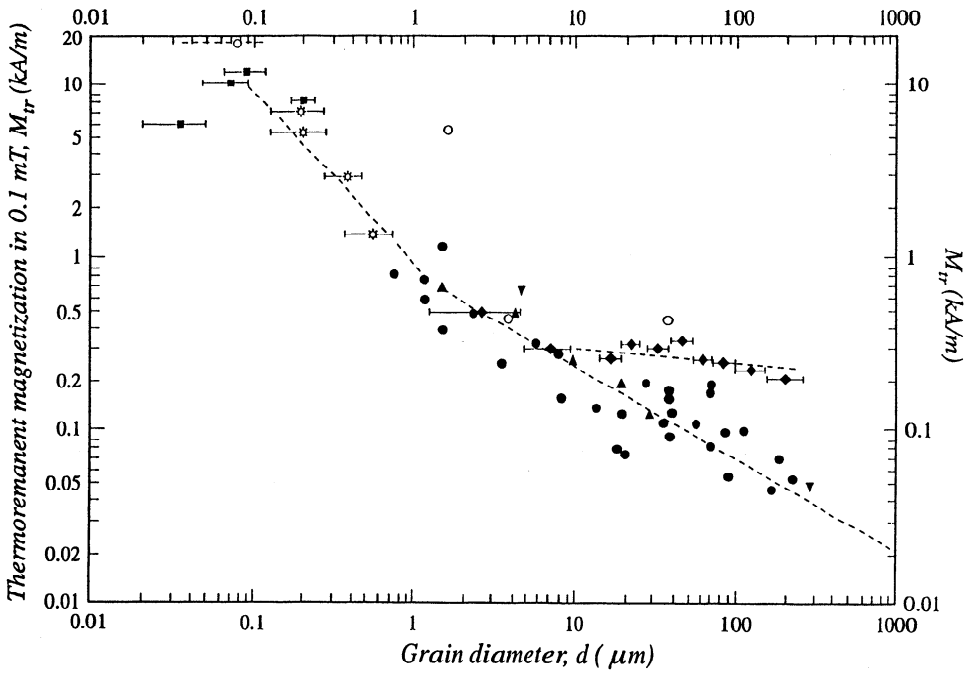

Figure 3. Experimental grain size dependence of weak field TRM intensity, M_{tr}, for magnetite. M_{tr} decreases approximately as 1/d between 0.1 and 10 μm. (After *Dunlop and Argyle* [1997], who identify the individual data points.)

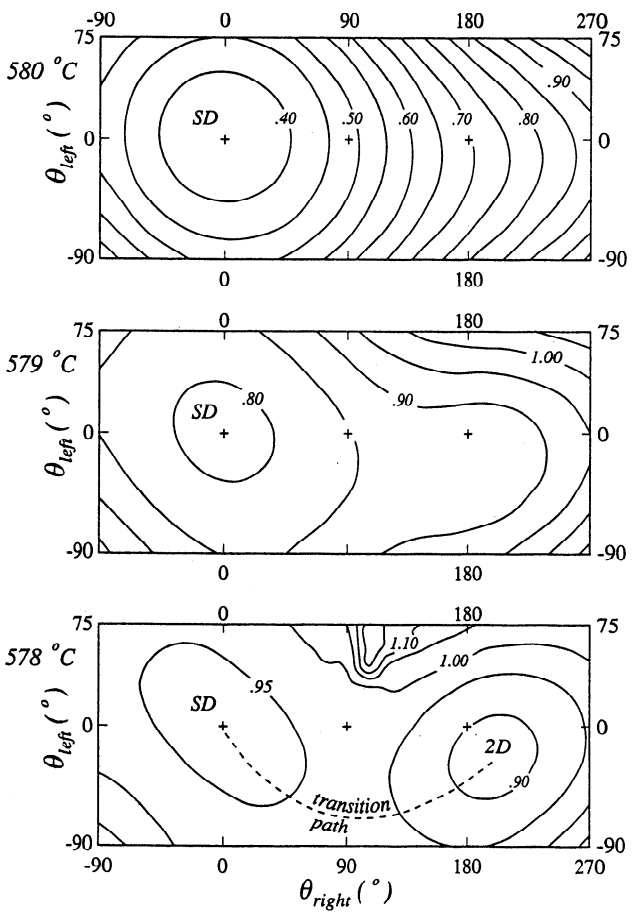

Figure 4. SD and 2D LEM states in magnetite at and just below T_C. Each LEM state is a local minimum on the total energy surface, here plotted as a function of spin angles at the left and right surfaces of a model magnetite grain of length 0.255 μm and elongation 1.5 (one-dimensional micromagnetic calculations, after *Dunlop et al.* [1994]). The transition path between states is the lowest energy route between the SD and 2D LEMs.

domain structure must be completely reconstituted. In this one-dimensional model, the transitional structures are easy to calculate and visualize: they correspond to nucleation of a domain wall at one edge of the grain and its propagation into the center (edge nucleation [see *Moon and Merrill*, 1985; *Dunlop et al.*, 1994]). The transdomain transition modes of two- and three-dimensional structures are not so easily found and in fact pose a major problem in predicting transdomain TRM.

Cooling further, we can follow the TRM blocking process (Figure 6). The energy wells and barriers shown are cross sections of the total energy surface taken along minimum-energy transition paths like the one shown in Figure 4. Building on SD theory, we note that a detailed knowledge of transitional structures is not necessary. We need only know the energies of the competing microstates, in this case, E_{SD} and E_{2D}, to find the thermal equilibrium Boltzmann partition between the states and thus the TRM intensity (compare equation (3)), and the peak energy E_{max} along the transition path, from which we can calculate the energy barriers ΔE_{12}, ΔE_{21} and hence the blocking temperature T_B. The latter calculation follows directly from equation (2). Blocking occurs when the relaxation time τ becomes equal to a typical experimental time t and so

$$\Delta E(T_B) = \ln(Ct)\, kT_B \quad \approx 25kT_B \quad t \approx 1 \text{ min}$$
$$\approx 60kT_B \quad t \approx 100 \text{ Ma.} \quad (4)$$

Of course, the exact numerical coefficient depends on the value of C, but there is no reason to believe the attempt frequency for transdomain transitions is greatly different from C for SD reversals.

At 574°C, the energy barriers to SD→2D and 2D→SD transitions are both <25kT. Transitions in both directions are frequent on ordinary timescales. Around 560°C, the 2D→SD barrier is still <25kT but the SD→2D barrier has grown to >60kT. Transitions into the SD state are easy on any time-

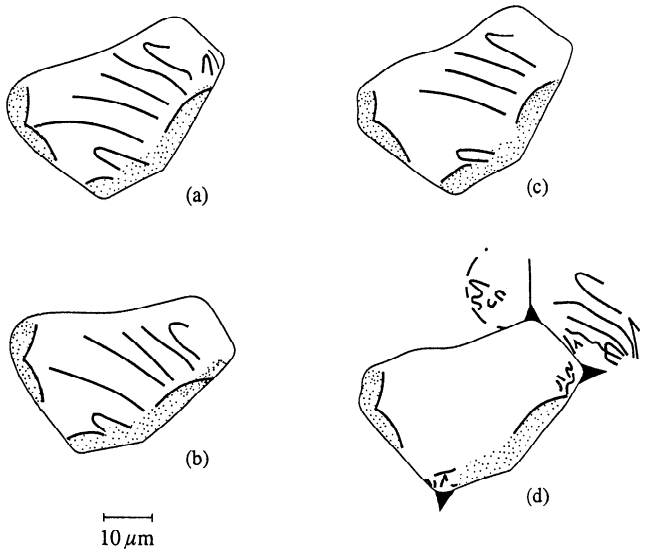

Figure 5. Four different domain structures observed in replicate TRM experiments on a 30 μm titanomagnetite grain: six lamellar domains with slightly different configurations (Figures 5a and 5b); five domains (Figure 5c); single domain (Figure 5d). (After *Halgedahl* [1991].)

scale, but transitions out of the SD state are prohibited even on geological timescales. We have reached the blocking temperature, and the Boltzmann probabilities p tell us that essentially all grains have blocked in the SD state. We could have reached the same conclusion from the kinetics alone.

In further cooling to 500°C, 2D becomes the GEM state and ΔE_{12} is now less than ΔE_{21}. However transitions to the 2D state are prohibited because both energy barriers are >>60kT. We have blocked a metastable SD TRM. Notice that because the energy difference between states is small ($E_{SD} - E_{2D} = 3kT$), the higher-energy SD state would have a small but significant population of short-term excitations (2.3%) if thermal equilibrium could be achieved.

5. Transdomain TRM: Prediction and Problems

The procedure we have just followed can be generalized to the blocking of transdomain TRM with any number and type of competing microstates. For example, consider the succession of two-dimensional micromagnetic states predicted for a 1 μm magnetite grain in Figure 7. The Monte Carlo modeling used [*Fukuma and Dunlop*, 1997] mimics the effect of thermal excitations and is very apt for simulating TRM.

The initial SD microstate (Figure 7a) evolves into a structure with four spin vortices, two counterclockwise on the left and two clockwise on the right (Figure 7b). Each vortex has a very small moment because of the circular spin structure, but the line of spins at the vortex center does have a moment, with a choice of orientations either into or out of the page. These vortex line moments have many features in common with SD moments, in particular, the two equivalent antiparallel microstates, which are independent of the surrounding vortex. However, vortex-line moments are very weak compared to the SD moment. They are also perpendicular to the SD structure (a) from which they evolved.

With further excitation, the left-hand and right-hand vortex pairs coalesce into elongated counterclockwise and clockwise vortices (Figure 7c). The central vortex line has now become a sheet with a much larger moment into or out of the page. This structure resembles and ultimately stabilizes into a conventional three-domain (3D) structure with four wedge-shaped closure domains at top and bottom (Figure 7d). These structures were first predicted by *Landau and Lifschitz*

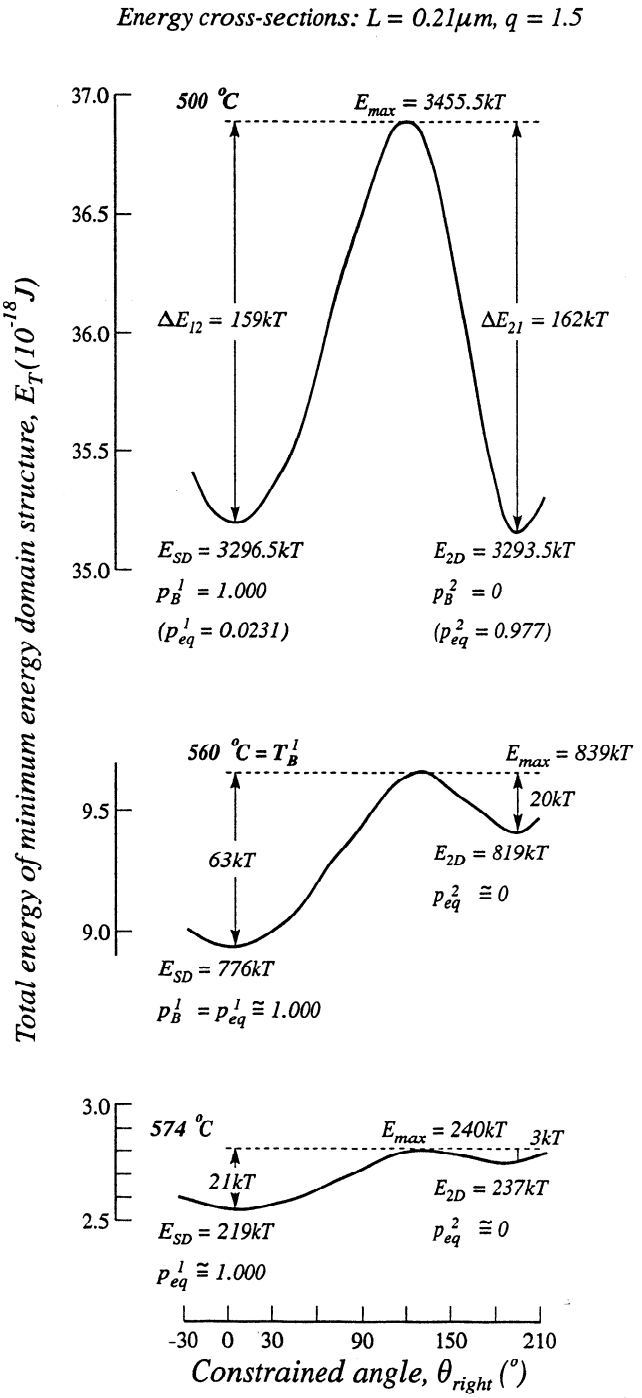

Figure 6. Theoretical energy cross sections along transition paths like the one in Figure 4 at three temperatures for a model magnetite grain of length 0.21 μm and elongation 1.5 [after *Dunlop et al.*, 1994]. Around 560°C, the energy barrier ΔE_{12} for transitions out of the SD state becomes >60kT. This is the blocking temperature T_B^1 for the SD state (the Boltzmann probability of the SD state is 1.000 at T_B^1). At 500°C, the 2D state becomes of lower energy, but the barriers ΔE_{12}, ΔE_{21} are >>60kT, preventing transitions. The grain therefore remains in a metastable SD state. Notice that the 3kT difference between 2D and SD energies results in an equilibrium Boltzmann probability of 0.977 for the favored (2D) state.

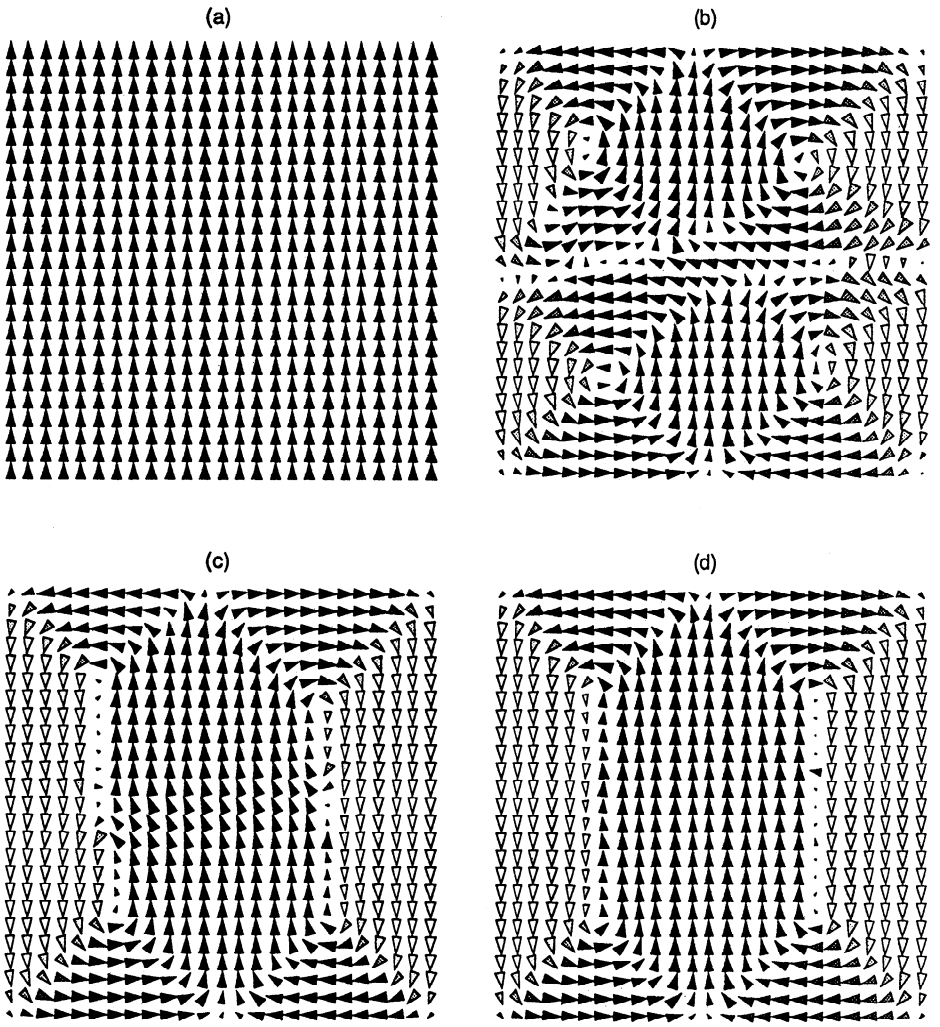

Figure 7. Calculated two-dimensional micromagnetic structures of a model 1 μm magnetite cube during Monte Carlo simulation of thermal excitations. (a) The initial SD structure evolves into (b) a 4-vortex state after 500 Monte Carlo steps (MCS), (c) a 2-vortex structure after 2000 MCS, and (d) ultimately into a lamellar 3-domain structure with 4 closure domains after 10,000 MCS. (After *Fukuma and Dunlop* [1997].)

[1935] and *Kittel* [1949] and have been clearly imaged in magnetite by *Özdemir et al.* [1995]. The "vortex sheets" are now recognizable as Bloch walls, with moments either into or out of the page. These domain wall moments (or "psarks" [*Dunlop*, 1977]) are perpendicular to the body domains (but not independent; *Pokhil and Moskowitz* [1997] show that wall moments reverse when the adjacent body domains reverse). Like vortex-line moments, wall moments are perpendicular to the initial SD moment (Figure 7a). However, wall moments are much larger than vortex-line moments.

The intermediate states in Figure 7 are not stable LEM states but resting states in the transformation from an SD to a 3D state. The 2D state (not shown) is not stable in a 1 μm magnetite grain but evolves into a single-vortex structure [*Fukuma and Dunlop*, 1997].

In order to predict transdomain TRM, we need the following information:

1. We require an enumeration of all possible remanence-carrying LEM states, which for a 1 μm magnetite grain, are SD and SD′, V and V′ (oppositely directed vortex moments), and 3D and 3D′ (oppositely directed pairs of wall moments; mutually cancelling wall moments are not of interest, although they are commonly observed [*Pokhil and Moskowitz*, 1997]).

2. We need also the energy E_i and net magnetization M_i (magnetic moment / grain volume) of each LEM state. The Boltzmann probability $p_i = \exp(-E_i/kt) / \Sigma \exp(-E_i/kT)$ determines the partitioning among microstates, and the thermal equilibrium magnetization (compare equation (3)) is

$$M_{eq} = \Sigma\, p_i M_i = \sum M_i \exp(-E_i/kT) / \sum \exp(-E_i/kT). \quad (5)$$

3. Finally, we must know the highest energy E_{max} encountered along the transition path (including resting states) between all pairs of LEM states. (Transition paths are unfortunately very difficult to compute except for the simplest structures [e.g., *Enkin and Williams*, 1994; *Fukuma and Dunlop*, 1997].) The energy barriers $\Delta E_{12} = E_{max} - E_1$, $\Delta E_{21} = E_{max} - E_2$ determine relaxation times and blocking temperatures for transitions between states 1 and 2 (compare equations (2) and (4)):

$$1/\tau_{12} = C_{12} \exp(-\Delta E_{12}/kT), \quad 1/\tau_{21} = C_{21} \exp(-\Delta E_{21}/kT), \quad (6)$$

$$\Delta E_{12}(T_{B12}) = \ln(C_{12}t)\, kT_{B12}, \quad \Delta E_{21}(T_{B21}) = \ln(C_{21}t)\, kT_{B21}. \quad (7)$$

In reality, for a particular pair of LEM states and a chosen

experimental time t, there is only one blocking temperature T_B, the higher of T_{B12} and T_{B21}. At T_B, provided the energy difference between E_1 and E_2 is $\geq 3kT$, the lower energy state is essentially 100% populated (compare Figure 6, top) and T_B for transitions out of the less favored state becomes irrelevant.

The kinetic equation is more complicated than equation (1) when there are more than two competing microstates. One must write a set of n equations, each describing the kinetics of transitions by all possible routes into and out of one of the n possible microstates [see *Moon and Merrill*, 1986]. However, just as in *Néel*'s [1949] SD theory, the details of the kinetics are unimportant in thermal processes because relaxation times change so enormously for small changes in T that transitions are either blocked or unblocked. If the set of possible LEM states does not change during cooling, there is only one blocking temperature T_B, namely, the highest of all the T_{B12} or T_{B21} values given by equation (7) for transitions between all possible pairs of competing states. Furthermore, at T_B the GEM state is essentially 100% populated and all other states are empty (see previous paragraph). TRM should therefore be blocked at a single T_B for all grains of a particular size, and all these grains should have the same magnetic microstate [*Dunlop et al.*, 1994].

This conclusion is contradicted by the observation that the same grain can occupy a variety of microstates when given replicate TRM's under identical conditions (Figure 5 [*Halgedahl*, 1991]). The flaw in our reasoning is unlikely to lie with the assumption of Boltzmann partitioning (equation (5)) or of thermal activation as a first-order rate process controlled by a single barrier energy E_{max} (equations (6) and (7)). It is true that the frequency factors C_{ij} may be different for different transdomain transformations, depending on the complexity of the transformation mode, but they are unlikely to vary by many orders of magnitude. In any case, modifications or refinements of any of these considerations would merely lead to another deterministic set of equations. The element of randomness evident in Figure 5 must originate elsewhere. We argued earlier that highly excited predomain states [*Ye and Merrill*, 1995] are unlikely to survive more than a degree or two below T_C. The flaw must lie in the assumption that the set of competing LEM states does not change during cooling.

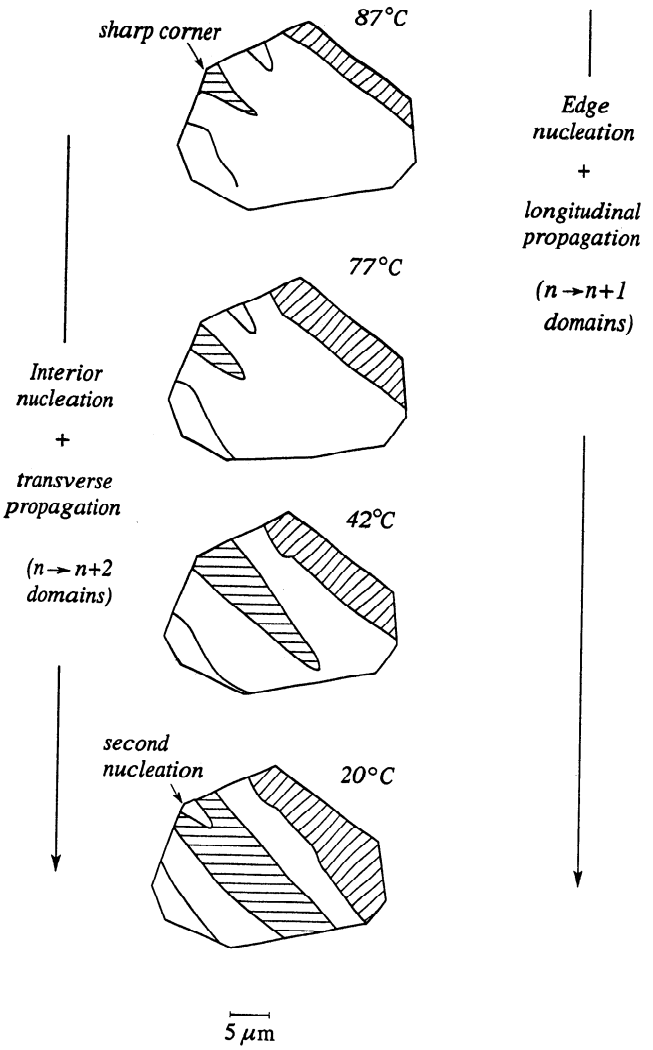

Figure 8. Experimental domain observations on a 30 μm magnetite crystal during cooling from above 100°C to room temperature [after *Heider et al.*, 1988]. Both edge nucleation and interior nucleation of domains occur during cooling.

6. Changes in Microstates During Cooling

Figure 8 illustrates several mechanisms by which magnetic microstates can change during cooling. A sharp corner in a 30 μm magnetite crystal acted as a nucleation site for a new spike domain during cooling from 87°C. Between 77 and 42°C, the spike propagated transversely across the crystal, transforming the original three-domain structure to a five-domain structure. A second nucleation occurred between 42 and 20°C at the same site. This same style of interior nucleation followed by transverse propagation of a spike domain is observed also in TM60 [*Halgedahl*, 1991].

A second type of domain nucleation in Figure 8 is the appearance of a lamellar body domain at the upper right face of the crystal, transforming the magnetic structure from two domains to three domains. This process of edge nucleation seems to be more difficult than interior nucleation. Between 87 and 20°C, the new domain propagated longitudinally into the crystal by successive Barkhausen jumps of its boundary (or sections of the boundary).

Domain boundary or wall displacement is a third mechanism of changing the magnetic microstate. It is much easier than either type of domain nucleation because the change in structure is minor compared to adding a new domain or transforming to or from a vortex state. Energy barriers are therefore quite low, and wall displacements occur readily during cooling for all domain walls, not just the boundaries of newly nucleated domains.

An important distinction is that in wall displacement there is a definite sequence of microstates traversed, whereas nucleation or other transdomain processes provide a set of simultaneous microstates between which direct transitions are possible. A 3D state, for example, can transform to 3D′ by reversing both wall moments, to vortex by transforming walls to vortices, to four domain by edge nucleation, to five domain by interior nucleation, to 2D by denucleating an edge domain, to SD by denucleating the central domain, and so on. In principle, all these microstates are simultaneously available and competing. Each wall in a structure with a fixed number of domains, on the other hand, propagates in a single Barkhausen jump only as far as the next pinning site of lower energy (see Figure 9). To reach a more distant microstate requires a sequence of jumps between adjacent states, with barriers of varying heights. The kinetics are multistage instead

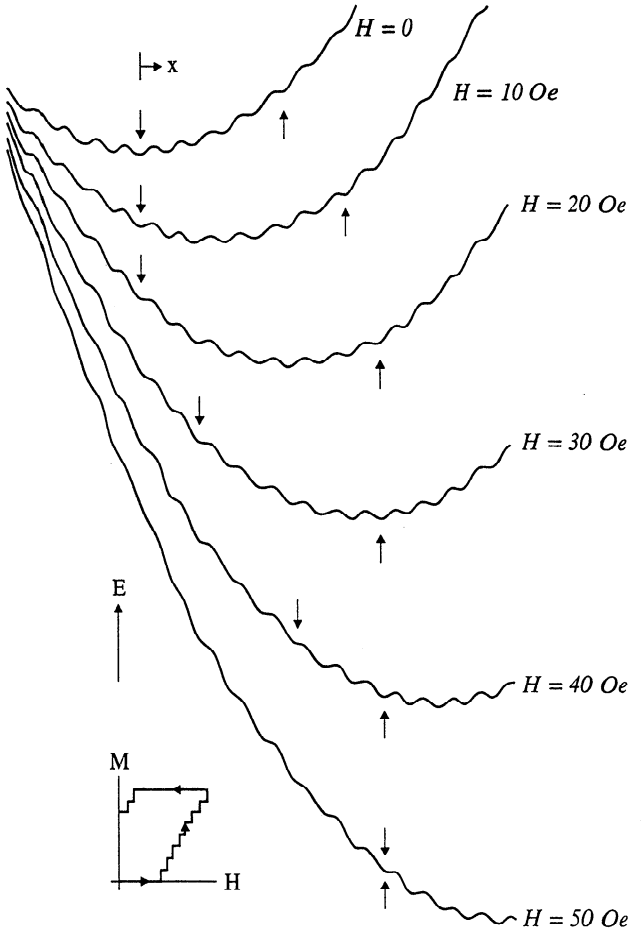

Figure 9. Total energy, $E_w + E_d + E_H$, as a function of wall displacement x from the center of a model magnetite grain [after *Schmidt*, 1973 with the kind permission of Elsevier Science - NL, Amsterdam, The Netherlands]. Successive wall positions in increasing fields (down arrows) are different from those in decreasing fields (up arrows) because of the asymmetry of energy wells and barriers. The grain is left with a displaced wall and a net remanence when H→0.

of single-stage and partitioning is correspondingly complex to calculate.

7. TRM Due to Wall Displacements

Néel [1955] proposed a theory of TRM based on equilibrium wall displacements, driven not by thermal excitations but by the changing internal demagnetizing field, $\mathbf{H_d} = -\mathbf{NM}$, where **M** is the local magnetization vector. Thermal activation of entire domain walls has prohibitively high energy barriers at all temperatures. Only segments of walls can be activated. $\mathbf{H_d}$, however, is a powerful field capable of driving entire walls at any temperature.

The process is illustrated in Figure 9. A domain wall is originally in the center of the grain, trapped in a local energy minimum (LEM) of the wall energy E_w created by interaction between the wall and lattice defects such as inclusions, voids, or dislocations [*Özdemir and Dunlop*, 1997]. The strength of trapping or pinning is determined by the barrier height between adjacent LEMs and is measured by the microcoercivity H_c. (H_c actually measures the steepest slope of the E_w barrier, which has a constant relation to height for barriers of a particular shape.) The central position is favored by the broad parabolic energy well arising from the demagnetizing energy E_d and expresses the restoring effect of $\mathbf{H_d}$. As the applied field **H** grows, the parabolas are tilted to the right by field energy E_H, "spilling" the wall from one LEM to another in a series of Barkhausen jumps. As the field decreases, the wall is pinned in a different set of LEMs because the barriers to wall motion are not symmetric in increasing and decreasing applied fields. As H→ 0, the wall remains trapped well away from the center of the grain, giving rise to a remanence, in this case an isothermal remanence.

TRM can be modeled in exactly the same way except that **H** is fixed and T changes. The amplitude of variations in E_w (i.e., H_c) decreases with T and so does the depth of the overall parabolic well due to self-demagnetization (i.e., H_d) but at different rates. If we start from high temperatures and cool, the wall is blocked in its jumps from right to left at a temperature T_B where the rates of change of H_c and of H_d with T become equal. At T_B, the growth in E_w barriers with cooling begins to outweigh the force of H_d pushing the wall back toward the demagnetized state and the wall is trapped. TRM has been blocked. However, in reheating in zero field from T_0, the wall makes a series of small jumps back to the central demagnetized LEM position, each driven by H_d. The jumps are small because E_w and therefore H_c decrease gradually with heating.

The essential conclusions of this field-blocking model are that TRM is acquired sharply at a single T_B during cooling [*Néel*, 1955] but demagnetizes gradually over a broad range from room temperature T_0 essentially to the Curie point T_C during zero-field heating (thermal demagnetization) [*Shcherbakov et al.*, 1993; *Dunlop and Xu*, 1994; *Xu and Dunlop*, 1994]. This asymmetry between TRM blocking and unblocking is in sharp contrast to SD TRM theory. It also has serious implications for paleomagnetism. There is no easy means of erasing a secondary thermal overprint of NRM held by pinned walls and isolating primary NRM. A thermal overprint acquired at temperature T_B in nature cannot be demagnetized by reheating the rock in the laboratory to a similar temperature, as with SD grains. Instead the rock must be heated to temperatures approaching T_C.

There are two main testable results of the *Néel* [1955] wall-pinning theory of TRM as extended by *Dunlop and Xu* [1994]. First, for fields larger than ≈0.5 mT, TRM intensity M_{tr} changes nonlinearly with applied field H_0:

$$M_{tr} = [n/(n-1)^{1-1/n}]\ \{[H_c(T_0)]^{1/n}/N\}\ H_0^{1-1/n}, \qquad (8)$$

where n is the coefficient in the temperature variation of H_c,

$$H_c(T) \propto M_s^n(T). \qquad (9)$$

Second, during zero-field heating, M_{tr} decreases quasi-continuously between T_0 and T_C, as

$$M_{tr}(T) \propto H_c(T) \propto M_s^n(T) \qquad (10)$$

for continuous thermal demagnetization (M_{tr} measured at T) or as

$$M_{tr}(T_0) \propto H_c(T)/M_s(T) \propto M_s^{n-1}(T) \qquad (11)$$

for stepwise thermal demagnetization (M_{tr} measured at T_0 after recooling from T). In very weak fields, Néel predicted a linear dependence of M_{tr} on H_0. However, this prediction is not quantitatively testable because the expression for M_{tr} contains

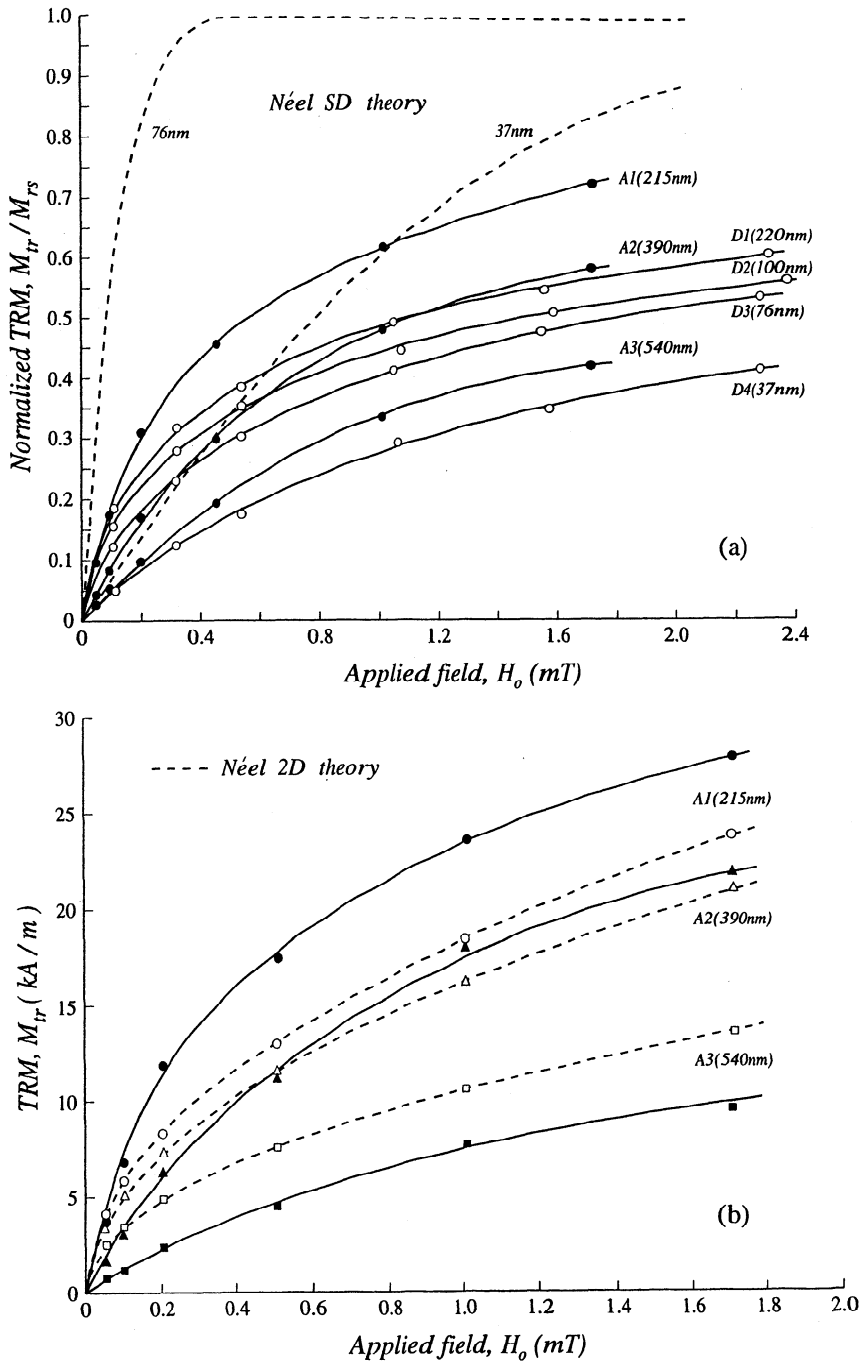

Figure 10. TRM intensity data as a function of applied field H_0 for SD and larger size magnetites [after *Dunlop and Argyle*, 1997]. (a) *Néel* [1949] SD theory does not predict the observed field dependence, even for SD (d≤ 100 nm) grains, but (b) *Néel* [1955] two-domain theory (field-blocked wall displacements) does match the observations for the larger grains.

experimentally inaccessible quantities related to the thermal fluctuation field at T_B (see discussion by *Dunlop and Xu* [1994]).

8. Experimental Tests

Among theories of TRM in nonuniformly magnetized grains, only the Néel theory of field-blocked wall displacements reviewed in section 7 is well enough developed to test quantitatively. (*Metcalf and Fuller* [1988] made a simple experimental test of metastable SD grains as carriers of TRM and showed that the dependence on applied field was reasonable, but such grains, although they have nonuniform states available (Figure 5), are only significant as remanence carriers when in their uniformly magnetized state.) Figure 10 compares theoretical predictions with experimental TRM field dependences for a number of synthetic magnetites ranging from SD size to about 0.5 μm. The *Néel* [1949] SD theory does not explain any of the data, not even for truly SD size grains (Figure 10a). The *Néel* [1955] 2D or wall-displacement

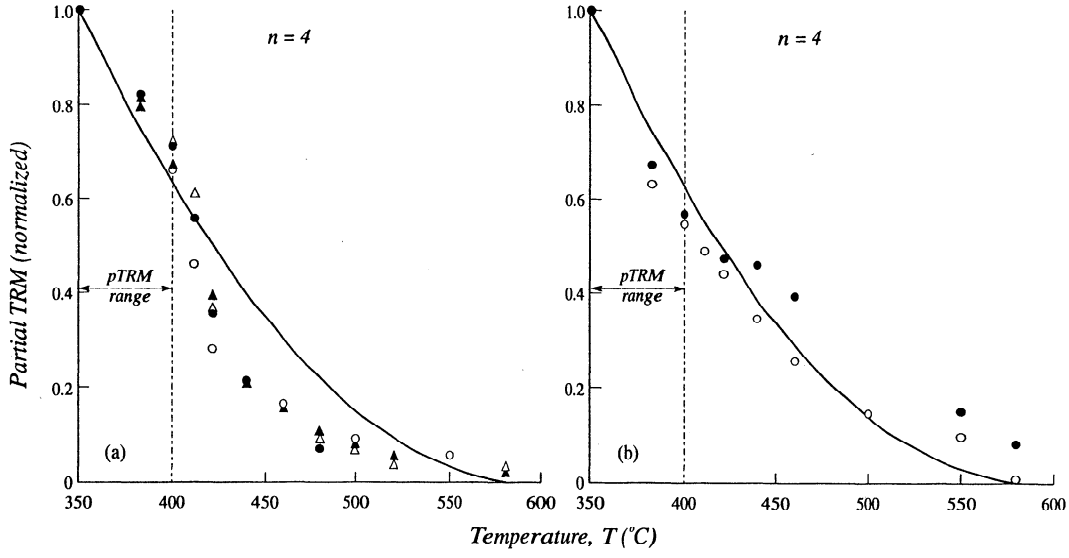

Figure 11. Theoretical fits (solid curves) to continuous thermal demagnetization data for partial TRMs of 3 μm and 40 μm magnetites [*Worm et al.*, 1988], using a value n= 4 in the theory of *Dunlop and Xu* [1994] and *Xu and Dunlop* [1994]. The agreement is good for the 40 μm grains but about 2/3 of the pTRM of the 3 μm grains demagnetizes just above the upper pTRM acquisition temperature of 400°C (SD-like behavior). (After *Xu and Dunlop* [1994].)

theory is more successful. Except in the very weak field region, it gives a reasonable match to observed absolute TRM intensities (Figure 10b).

It is possible to fine tune such theoretical fits by combining SD and multidomain theories [see, e.g., *Dunlop and Argyle*, 1997]. The rationale is that grains larger than SD size may have microstructures that permit both SD-like and MD-like responses to changing fields and temperatures (pseudo-SD or PSD behavior). An example is the three-domain structure (Figure 7d). Wall displacements result in magnetizations directed up or down, parallel to the main domains, but wall moments directed into or out of the page give SD-like magnetizations. Another example is a mixture of states like those in Figure 5. Some grains contain walls, while others of similar size are (metastably) SD. Actual quantitative fits to observed TRM field dependences are quite successful but mainly give information about the SD part of the remanence [*Dunlop and Argyle*, 1997] and will not be considered further here.

A test of the thermal demagnetization predictions of wall-displacement theory appears in Figure 11. The data are for continuous thermal demagnetization of partial TRM's acquired in field cooling from 400 to 350°C by 3 μm and 40 μm magnetite grains [*Worm et al.*, 1988]. In the case of partial TRM's, equations (10) and (11) are still valid, but demagnetization begins at the lower pTRM acquisition temperature (350°C) rather than at T_0 as with total TRM [*Dunlop and Xu*, 1994; *Xu and Dunlop*, 1994]. The fit to observations is quite good for the 40 μm grains but about 2/3 of the pTRM of the 3 μm grains demagnetizes quite sharply at or just above the upper pTRM acquisition temperature (400°C) in SD fashion. The remaining 1/3 of the pTRM tails off in the predicted fashion to T_C (580°C). Thus 3 μm magnetites have a PSD mixture of SD and MD responses, but 40 μm grains have a purely multidomain TRM, at least with respect to thermal demagnetization.

Figure 12 is a further illustration of the difference between the $T_B = T_{UB}$ behavior of SD grains and the $T_B \neq T_{UB}$ spectrum of T_{UB} behavior of pinned walls in multidomain grains. The samples are plagioclase and dark mineral separates from a diabase dike. The plagioclase contains elongated submicroscopic needles of magnetite and is an excellent example of SD material. The dark minerals, particularly biotite, contain very coarse-grained magnetite with typically MD hysteresis parameters. Partial TRM is acquired (at T_B) and thermally erased (at T_{UB}) in a perfectly reciprocal fashion by the plagioclase: the pTRM acquisition and "NRM" (here laboratory total TRM) thermal demagnetization curves are exact mirror images. Each pTRM fraction unblocks sharply, in SD fashion, with $T_{UB} = T_B$. For the dark minerals, pTRM acquisition is slower (i.e., concentrated at higher temperatures), and thermal demagnetization is more rapid than for the plagioclase, although it also continues to very high temperatures.

This asymmetry between TRM or pTRM acquisition and its subsequent thermal demagnetization causes nonideal behavior in Thellier paleointensity determination [see *Perrin*, this issue]. Partial TRM acquisition and NRM demagnetization curves like those of Figure 12 can be combined in a single plot, with T as a parameter (Figure 13). Because SD grains have symmetrical curves, NRM lost in zero-field heating to T is exactly replenished by pTRM gained during in-field heating/cooling to the same T, so that the NRM versus pTRM graph is linear. Multidomain TRM is lost more quickly and pTRM is gained more slowly than SD TRM or pTRM (Figure 12), with the result that the NRM versus pTRM graph sags below the ideal SD line. The sagging increases steadily as grain size increases for a set of crushed and annealed magnetites (Figure 13). For the largest grains, the curvature is extreme and agrees reasonably well with predictions based on multidomain field blocking theory [*Dunlop and Xu*, 1994].

9. Discussion

Theories of TRM are well developed for grains with simple microstructures: SD (including metastable SD), multidomain (MD) with an unchanging number of mobile walls, and hybrids of these two (simple PSD models). Since SD TRM is quite intense, even in weak fields (equation (3); theoretical SD

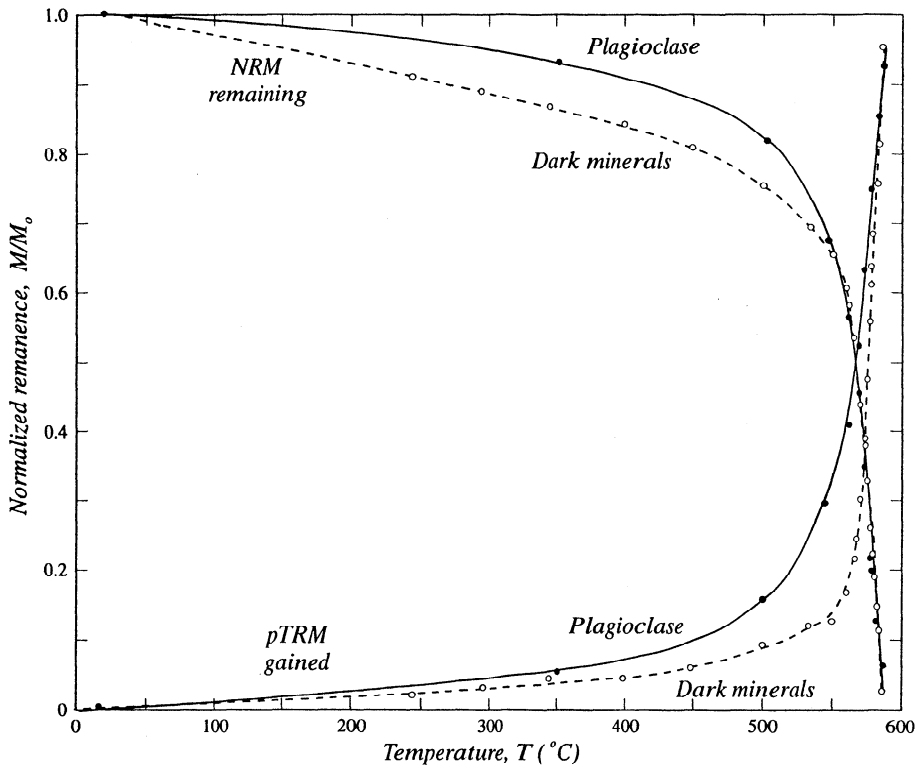

Figure 12. Stepwise acquisition of partial TRM and thermal demagnetization of "NRM" (a laboratory TRM) for two mineral separates from a diabase dike (courtesy of B. Zhang). The plagioclase has SD behavior: the pTRM and NRM curves are mirror images. The dark minerals have MD behavior: both pTRM and NRM curves fall below their SD counterparts (D.J. Dunlop and Ö. Özdemir, unpublished data, 1996).

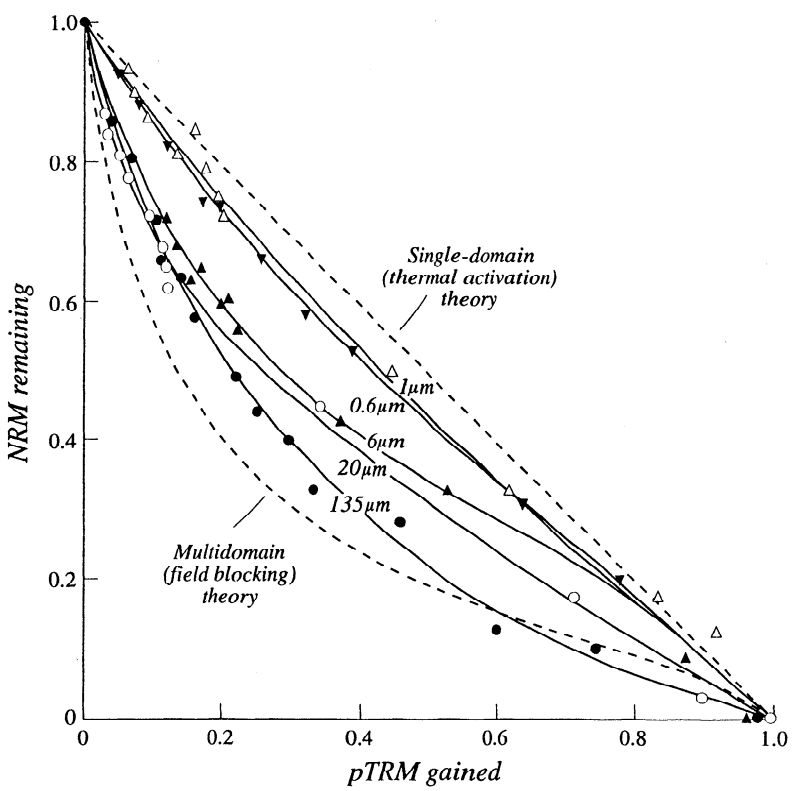

Figure 13. Simulated paleointensity determination, using laboratory TRM as NRM, for sized magnetites. With increasing grain size, the data deviate increasingly from the ideal single-domain line toward the predictions of multidomain field-blocking theory [*Dunlop and Xu*, 1994] (S. Xu and D.J. Dunlop, unpublished data, 1995).

curves, Figure 10a), whereas MD TRM is weak by comparison (equation (8); Figure 10b), it is possible to explain the grain size dependence of TRM intensity (Figure 3) in an ad hoc fashion as due to mixtures of SD (or metastable SD) and nonuniformly magnetized grains, or parts of grains. Various PSD models are able to generate an ~1/d dependence of M_{tr} over limited ranges of grain size [see, e.g., *Dunlop*, 1986] or *Dunlop and Özdemir*, 1997, Chapter 12], but none covers the entire broad size range of Figure 3, from ~0.1 μm to ~10 μm or possibly 100 μm in magnetite and corresponding ranges in other minerals. Furthermore, none of the simple PSD models takes into account vortex structures, which are predicted by all micromagnetic calculations to be the GEM state in magnetite just above d_0 [*Schabes and Bertram*, 1988; *Williams and Dunlop*, 1990, 1995; *Newell et al.*, 1993; *Enkin and Williams*, 1994; *Fabian et al.*, 1996], or other microstructures that deviate significantly from conventional Kittel or Landau-Lifschitz lamellar domain structures.

Vortex-line moments have two possible orientations, both perpendicular to the main spin structure, and can be treated theoretically by adapting *Néel* [1949] SD theory. So too can the moments of domain walls. In either case, however, one has the problem that these moments are very small compared to the moment of the whole grain in an SD state. The problem is particularly acute for vortex moments, which should produce a TRM about 1% that of SD TRM. If the main competing states near d_0 are SD and vortex, as micromagnetic models predict, there should be a drop of 1-2 orders of magnitude in M_{tr} around this size. This abrupt plummet is not seen experimentally.

One possible explanation is that metastable SD states can occur in grains very much larger than critical SD size, contrary to micromagnetic predictions, and that they overshadow all other sources of TRM. Metastable SD states certainly occur in pyrrhotite and TM60 grains >>1 μm in size (e.g., Figure 5), although their presence in magnetite grains of similar size is less well documented. In this case, the presence or absence of vortex states would be irrelevant to TRM. Recent experimental evidence implies that the situation is even more complicated, however. In magnetites of most grain sizes, the intensities of TRM and of anhysteretic remanent magnetization (ARM) are similar, but in magnetites with sizes just above d_0, TRM is 10-20 times more intense than ARM [*Dunlop and Argyle*, 1997]. The interpretation given by Dunlop and Argyle is that vortex states do not contribute significantly to TRM in magnetites of this size, but the strong alternating fields used in ARM production nucleate vortex structures at the expense of other states, including 2D and metastable SD.

Transdomain changes of this sort are particularly interesting because, depending on the nucleation mode, vortex or 2D wall moments may be perpendicular to the SD moment of their transdomain partner state (compare Figure 7). Transdomain TRM thus has the potential to change the direction as well as the intensity of magnetization.

The formalism for dealing quantitatively with transdomain TRM partitioned among any number of competing microstates is given in equations (5)-(7). However, to date no quantitative predictions have actually been made of transdomain TRM. There are two main problems. First, the minimum-energy transformation mode, or the transition path in a configuration space like that of Figure 4, is extremely difficult to find for any but the simplest pairs of LEM states (e.g., SD and vortex [*Enkin and Williams*, 1994]). Monte Carlo or simulated annealing algorithms imitate the effect of thermal excitations, but they are very time consuming and expensive. Semiconstrained transformations [e.g., *Dunlop et al.*, 1994; *Enkin and Williams*, 1994] are more economical but may not locate the saddle-point of energy E_{max} on the transition path. A small error in barrier energy can mean an enormous error in calculating transition probabilities and relaxation times, because of the exponential dependence on energy (equations (2), (6)).

A second and equally serious problem is that the Boltzmann energetics are such that the GEM state should be virtually 100% populated at the blocking temperature T_B. There should be no choice of microstates and thus effectively no transdomain TRM. This prediction clearly runs counter to the experimental evidence that replicate TRMs have different structures (Figure 5). The explanation is simple. The partitioning among LEM states changes with cooling because some states become unstable and others are added to the set. This is a difficult problem to deal with because of the complexity and number of competing LEM states in larger grains, but there is no doubt that it occurs. Domain observations made during cooling are decisive (Figure 8 [see also *Halgedahl*, 1991]). Independent evidence comes from changes in total and partial TRMs measured during cooling (rather than at T_0 following cooling) which are most naturally explained by transdomain changes, i.e., the nucleation or denucleation of one or more domains [see, e.g., *McClelland and Sugiura*, 1987]. Observations of this type are discussed by *McClelland et al.* [1996].

The shift in the set of competing LEM states as T decreases means that there are effectively many successive blocking temperatures. Only the lowest of these, after all possible transdomain changes have ceased, is really significant, because each domain nucleation or denucleation alters the internal demagnetizing field $\mathbf{H_d}$ and causes previously pinned walls to move. If transdomain changes in TRM typically continue to quite low temperatures, for example, ≤100°C as in Figure 8, even mild reheating of MD grains at some later time would probably cause further restructuring. The result would be massive remagnetization in nature. Until this speculation can be disproven, we should follow conventional paleomagnetic wisdom and mistrust NRMs carried by large MD grains.

10. Conclusions

1. *Néel*'s [1949] theory of TRM and pTRM in SD grains as a partition between competing microstates provides a good first order model of remanence blocking and unblocking, although the intensity of TRM is not quantitatively predicted (Figure 10a).

2. Near and above the SD threshold size, the set of competing microstates includes alternative LEM states like SD, vortex, and lamellar structures with closure domains.

3. TRM is blocked when transitions between all possible pairs of competing states cease. The transdomain blocking criterion is similar to the SD one: energy barriers between states must grow to $25kT_B - 60kT_B$ (laboratory to geological timescales).

4. At blocking, only the lowest energy LEM state (the GEM state) should be significantly populated (Figure 6). Transdomain TRM should have a single T_B for a given grain size and little or no choice of structure.

5. However, experimental observations show that grains do have a choice of structures in TRM (Figure 5) and that transdomain changes in structure, involving edge and interior nucleation of domains, continue during cooling, even near T_0 (Figure 8).

6. Barkhausen jumps of walls, driven by the internal demagnetizing field $\mathbf{H_d}$, occur much more readily than nucleation of new walls and form the basis of *Néel*'s [1955]

theory of TRM in MD grains. Néel's prediction of TRM intensity as a function of applied field strength H_0 is supported by data on magnetites ≤ 0.5 μm in size (Figure 10b).

7. Thermal demagnetization of MD TRM is gradual and occurs by many successive small jumps of pinned walls. Thermal demagnetization data and simulated paleointensity determinations for MD magnetites are well explained by *Dunlop and Xu*'s [1994] extension of the *Néel* [1955] theory (Figures 11 and 13).

8. Transdomain changes in TRM during cooling and gradual unblocking of any MD TRM during zero-field heating have serious implications for NRM acquisition and remagnetization in nature. MD grains may acquire thermal overprints rather easily but these secondary NRMs can only be completely erased by heating nearly to T_C.

9. Our greatest advances in understanding TRM since the time of *Néel* [1949] and *Kittel* [1949] have been in the discovery of alternative structures (LEM states) of individual crystals and their exploration in detail through micromagnetic calculations. However, quantitative theories of transdomain TRM will require accurate tracing of transition paths between LEM states and a better understanding of how and why domains nucleate at low temperatures during cooling.

Acknowledgments. Many colleagues have helped shape my understanding of TRM, although they do not necessarily share all my views. In particular, I thank Ken Argyle, Subir Banerjee, Randy Enkin, Mike Fuller, Sue Halgedahl, Buffy McClelland, Ron Merrill, Özden Özdemir, Michel Prévot, Valera Shcherbakov, Frank Stacey, Wyn Williams, and Song Xu. Careful reviews by Bruce Moskowitz and an anonymous referee raised a number of interesting points that clarified the paper. This research has been supported by NSERC grant A7709.

References

Boyd, J.R., M. Fuller, and S. Halgedahl, Domain wall nucleation as a controlling factor in the behaviour of fine magnetic particles in rocks, *Geophys. Res. Lett., 11*, 193-196, 1984.

Dunlop, D.J., The hunting of the "psark", *J. Geomagn. Geoelectr., 29*, 293-318, 1977.

Dunlop, D.J., Hysteresis properties of magnetite and their dependence on particle size: A test of pseudo-single-domain remanence models, *J. Geophys. Res., 91*, 9569-9584, 1986.

Dunlop, D.J., and K.S. Argyle, Thermoremanence, anhysteretic remanence, and susceptibility of submicron magnetites: Nonlinear field dependence and variation with grain size, *J. Geophys. Res., 102*, 20,199-20,210, 1997.

Dunlop, D.J., and Ö. Özdemir, *Rock Magnetism: Fundamentals and Frontiers*, 573 pp., Cambridge Univ. Press, New York, 1997.

Dunlop, D.J., and S. Xu, Theory of partial thermoremanent magnetization in multidomain grains, 1, Repeated identical barriers to wall motion (single microcoercivity), *J. Geophys. Res., 99*, 9005-9023, 1994.

Dunlop, D.J., A.J. Newell, and R.J. Enkin, Transdomain thermoremanent magnetization, *J. Geophys. Res., 99*, 19,741-19,755, 1994.

Enkin, R.J., and D.J. Dunlop, A micromagnetic study of pseudo single-domain remanence in magnetite, *J. Geophys. Res., 92*, 12,726-12,740, 1987.

Enkin, R.J., and W. Williams, Three-dimensional micromagnetic analysis of stability in fine magnetic grains, *J. Geophys. Res., 99*, 611-618, 1994.

Fabian, K., A. Kirchner, W. Williams, F. Heider, T. Leibl, and A. Hubert, Three-dimensional micromagnetic calculations for magnetite using FFT, *Geophys. J. Int., 124*, 89-104, 1996.

Fukuma, K., and D.J. Dunlop, Monte Carlo simulation of two-dimensional domain structures in magnetite, *J. Geophys. Res., 102*, 5135-5143, 1997.

Halgedahl, S.L., Magnetic domain patterns observed on synthetic Ti-rich titanomagnetite as a function of temperature and in states of thermoremanent magnetization, *J. Geophys. Res., 96*, 3943-3972, 1991.

Halgedahl, S.L., and M. Fuller, The dependence of magnetic domain structure upon magnetization state with emphasis upon nucleation as a mechanism for pseudosingle domain behaviour, *J. Geophys. Res., 88*, 6505-6522, 1983.

Heider, F., S.L. Halgedahl, and D.J. Dunlop, Temperature dependence of magnetic domains in magnetite crystals, *Geophys. Res. Lett., 15*, 499-502, 1988.

Kittel, C., Physical theory of ferromagnetic domains, *Rev. Mod. Phys., 21*, 541-583, 1949.

Landau, L.D., and E.M. Lifschitz, On the theory of the dispersion of magnetic permeability in ferromagnetic bodies, *Phys. Z. Sowjetunion, 8*, 153-169, 1935.

McClelland, E., and N. Sugiura, A kinematic model of TRM acquisition in multidomain magnetite, *Phys. Earth Planet. Inter., 46*, 9-23, 1987.

McClelland, E., A.R. Muxworthy, and R.M. Thomas, Magnetic properties of the stable fraction of remanence in large multidomain (MD) magnetic grains: Single-domain or MD? *Geophys. Res. Lett., 23*, 2831-2834, 1996.

Metcalf, M., and M. Fuller, A synthetic TRM induction curve for fine particles generated from domain observations, *Geophys. Res. Lett., 15*, 503-506, 1988.

Moon, T., and R.T. Merrill, The magnetic moments of non-uniformly magnetized grains, *Phys. Earth Planet. Inter., 34*, 186-194, 1984.

Moon, T., and R.T. Merrill, Nucleation theory and domain states in multidomain material, *Phys. Earth Planet. Inter., 37*, 214-222, 1985.

Moon, T., and R.T. Merrill, A new mechanism for stable viscous remanent magnetization and overprinting during long magnetic polarity intervals, *Geophys. Res. Lett., 13*, 737-740, 1986.

Néel, L., Théorie du traînage magnétique des ferromagnétiques en grain fins avec applications aux terres cuites, *Ann. Géophys., 5*, 99-136, 1949.

Néel, L., Some theoretical aspects of rock magnetism, *Adv. Phys., 4*, 191-242, 1955.

Newell, A.J., D.J. Dunlop, and W. Williams, A two-dimensional micromagnetic model of magnetizations and fields in magnetite, *J. Geophys. Res., 98*, 9533-9549, 1993.

Özdemir, Ö., and D.J. Dunlop, Effect of crystal defects and internal stress on the domain structure and magnetic properties of magnetite, *J. Geophys. Res., 102*, 20,211-20,224, 1997.

Özdemir, Ö., S. Xu, and D.J. Dunlop, Closure domains in magnetite, *J. Geophys. Res., 100*, 2193-2209, 1995.

Perrin, M., Paleointensity determination, magnetic domain structure, and selection criteria, *J. Geophys. Res.*, this issue.

Pokhil, T.G., and B.M. Moskowitz, Magnetic domains and domain walls in pseudo-single-domain magnetite studied with magnetic force microscopy, *J. Geophys. Res., 102*, 22,681-22,694, 1997.

Sahu, S., and B.M. Moskowitz, Thermal dependence of magnetocrystalline anisotropy and magnetostriction constants of single crystal $Fe_{2.4}Ti_{0.61}O_4$, *Geophys. Res. Lett., 22*, 449-452, 1995.

Schabes, M.E., and H.N. Bertram, Magnetization processes in ferromagnetic cubes, *J. Appl. Phys., 64*, 1347-1357, 1988.

Schmidt, V.A., A multi-domain model of thermoremanence, *Earth Planet. Sci. Lett., 20*, 440-446, 1973.

Shcherbakov, V.P., E. McClelland, and V.V. Shcherbakova, A model of multidomain thermoremanent magnetization incorporating temperature-variable domain structure, *J. Geophys. Res., 98*, 6201-6216, 1993.

Williams, W., and D.J. Dunlop, Some effects of grain shape and varying external magnetic field on the magnetic structure of small grains of magnetite, *Phys. Earth Planet. Inter., 65*, 1-14, 1990.

Williams, W., and D.J. Dunlop, Simulation of magnetic hysteresis

in pseudo-single-domain grains of magnetite, *J. Geophys. Res., 100*, 3859-3871, 1995.

Worm, H.-U., M. Jackson, P. Kelso, and S.K. Banerjee, Thermal demagnetization of partial thermoremanent magnetization, *J. Geophys. Res., 93*, 12,196-12,204, 1988.

Xu, S., and D.J. Dunlop, Theory of partial thermoremanent magnetization in multidomain grains, 2, Effect of microcoercivity distribution and comparison with experiment, *J. Geophys. Res., 99*, 9025-9033, 1994.

Ye, J., and R.T. Merrill, Use of renormalization group theory to explain the large variation of domain states observed in titanomagnetites and implications for paleomagnetism, *J. Geophys. Res., 100*, 17,899-17,907, 1995.

D. J. Dunlop, Geophysics, Physics Department, University of Toronto, Toronto, Ontario, Canada M5S 1A7. (e-mail: dunlop@physics.utoronto.ca)

(Received June 6, 1997; revised December 2, 1997; accepted December 23, 1997.)